Mechanism of Enhanced Cellular Uptake and Cytosolic Retention of MK2 Inhibitory Peptide Nano-polyplexes

By

Kameron V. Kilchrist

Thesis
Submitted to the Faculty of the
Graduate School of Vanderbilt University
in partial fulfillment of the requirements
for the degree of

MASTER OF SCIENCE
in

Biomedical Engineering
May 2016
Nashville, Tennessee

Approved:
Craig L. Duvall, Ph.D.
Hak-Joon Sung, Ph.D.

ACKNOWLEDGEMENTS

I thank Dr. Brian Evans, Ph.D., Dr. Colleen Brophy, M.D., and Dr. Craig Duvall, Ph.D. for their guidance, support, and contributions in preparing this work. I thank Dr. Felix Randow and Dr. Bob Weinburg for kind gifts of plasmids via AddGene.com and Dr. Janice Williams for imaging support and electron microscopy expertise, without whom this work would not be possible. Confocal imaging, transmission electron microscopy, and scanning electron microscopy were performed in part through the use of the Vanderbilt University Medical Center Cell Imaging Shared Resource (supported by NIH grants CA68485, DK20593, DK58404, DK59637 and EY08126). Dynamic light scattering was conducted at the Vanderbilt Institute of Nanoscale Sciences and Engineering. This work was supported by the American Heart Association (11SDG4890030), National Institutes of Health / National Heart, Lung, and Blood Institute (1R21HL110056), and a National Science Foundation Graduate Research Fellowship to K.V.K. (0909667 and 1445197).

TABLE OF CONTENTS

LIST OF TABLES

Table **Page**

LIST OF FIGURES

INTRODUCTION

Intracellular-acting peptides have the potential to be applied as powerful research tools to modulate kinase activity, alter protein-protein interactions, and elucidate specific protein functions[6,28,32,45]. Peptides can modulate targets not druggable by conventional small molecules and can be rationally designed to have more predictable and specific activity. However, clinical use of peptides is limited due to lack of intracellular bioavailability. This lack of bioavailability arises because peptides are too large and hydrophilic to diffuse across cell membranes. To overcome this barrier, the majority of peptides used in research are modified with cationic cell penetrating peptides (CPPs) to facilitate plasma membrane transduction[14,16,24]. Initial reports suggested that some CPPs may directly translocate the cell membrane, but later studies[39] showed this effect to be an artefact of microscopy. Upon endocytosis, CPPs typically traffic through early and late endosomes before ultimately becoming entrapped in lysosomes[22,27], sequestering a large portion of the drug away from its intracellular binding target. Many research groups have used polymeric nano-carriers to enable endo-lysosomal escape of biologic drugs like nucleic acids and peptides[12,17]. Although debated, the 'proton sponge' mechanism of endosomal escape has been extensively described for nucleic acid delivery systems like polyethyleneimine[2,7]; however, the effects of endosomal escape on the subsequent trafficking of the drug cargo remain unclear[44]. Anionic, pH-responsive carriers like the one described herein have been shown to reduce trafficking into acidifying compartments following CD22-dependent receptor mediated uptake[3]. While the pharmacodynamics of anionic, polymer-based nano-polyplexes (NPs) used for the delivery of both an intracellular acting MAPKAP kinase 2 inhibitory (MK2i) peptide and a peptide mimetic of phosphorylated heat shock protein 20 (p-HSP20) have been thoroughly investigated [18,19], the mechanisms and kinetics of NP uptake and trafficking have not been rigorously studied.

The current studies focus on the comprehensive analysis of an established MK2i-NP formulation, which our group previously developed for the cytosolic delivery of MK2i to vascular smooth muscle cells to prevent intimal hyperplasia and vasospasm[18,19]. A previous study on a therapeutic peptide fused to a CPP by Flynn et al. found that the AZX100 peptide, which comprises the same CPP sequence as MK2i and p-HSP20, was internalized rapidly *via* a lipid raft dependent, caveolae mediated uptake process that was not significantly influenced by actin or dynamin inhibition. This work demonstrated that the majority of internalized peptide was sequestered within the endo-lysosomal system, preventing the peptide from efficiently binding to its target intracellular[22]. Upon phosphorylation, MK2 is translocates from the nucleus to the cytosol, where it phosphorylates downstream mediators in the p38/MAPK signaling axis[30,35]; MK2i binds to and blocks the active site used by MK2 to phosphorylate these downstream mediators[25,33]. MK2i-NPs[18,19], formed by the simple mixing of the cationic MK2i peptide with the anionic, endosomolytic polymer poly(propylacrylic acid) (PPAA) at pH 8, are electrostatically complexed nano-sized structures with a negative zeta potential ($\zeta\sim$ -12 mV). In contrast to the traditional dogma within the biomacromolecular drug delivery field that cationic charge should be utilized to enhance intracellular delivery of CPPs[26], polymeric micelles[13,15], and lipoplexes[21], formulation into negatively charged NPs significantly enhances the cellular uptake of CPP-based peptides (e.g., both MK2i and p-HSP20)[19],. MK2i-NPs demonstrate a longer duration of intracellular retention relative to free MK2i and demonstrated equivalent bioactivity at an order of magnitude lower dose than the free peptide or control, non-endosomolytic nano-polyplexes formed with poly(acrylic acid) (PAA)[18,19]. Both PPAA and PAA contain pH-responsive carboxylate moieties that drive electrostatic complexation with cationic MK2i peptide, however, due to the α-alkyl substitution of a pendant propyl chain, the carboxylate of PPAA has an effective acid dissociation constant (pK_a)

of ~6.8 (whereas the pK_a of the pendant carboxylate of PAA is ~4.3). This difference results in PPAA, but not PAA, demonstrating pH-dependent membrane disruptive activity at pH values encountered during endo-lysosomal trafficking (i.e., pH 4.5 – pH 7.4) [41]. Although formulation with either polymer at an optimized charge ratio formed NPs with statistically equivalent size and surface charge, control NPs formulated with non-endosomolytic PAA did not enhance cellular uptake or bioactivity. These findings motivated exploration into how the physicochemical properties of PPAA-based MK2i-NPs affect uptake, cellular processing, and intracellular trafficking of the therapeutic MK2i payload. Understanding the cellular mechanisms underlying the enhanced cellular uptake and altered cellular trafficking of MK2i-NPs may provide insights generalizable to intracellular delivery of peptides and other biomacromolecular drugs.

MATERIALS AND METHODS

Materials

Poly(propylacrylic acid) and MK2i were synthesized as previously reported[18,19]. MK2i-NPs were formulated (**Fig. 1a**) and characterized as previously described[18]. Endocytic inhibitors were obtained from Sigma-Aldrich. MK2i peptide was labeled with Alexa 488-NHS or Alexa 568-NHS (ThermoFisher Scientific) according to manufacturer instructions and purified with a desalting column (PD10 Miditrap, GE). Conjugation efficiency and conjugate purity were verified by UV-VIS spectroscopy. Fluorescently labeled MK2i peptide was used to formulate fluorescently labeled MK2i-NPs. To formulate gold labeled MK2i-NPs (Au-MK2i-NPs), a solution of 10 nm gold nanoparticles stabilized in PBS (Sigma-Aldrich 752584) was first added to PPAA, to which MK2i was subsequently added. Au loading into MK2i-NPs was confirmed by the complete disappearance of the 10 nm gold peak in DLS measurements.

Cell Culture

Cell culture reagents were purchased from Gibco/Thermo Fisher Scientific (Waltham, MA, USA) unless otherwise specified. Human coronary artery vascular smooth muscle cells were obtained from Lonza and grown in ATCC Vascular Cell Basal Medium supplemented with ATCC Vascular Smooth Muscle Cell Growth Kit (ATCC, Manassas, VA, USA), 1% Penicillin-Streptomycin, and Plasmocin prophylactic (Invivogen, San Diego, CA USA). All cultures were maintained in 75cm^2 polystyrene tissue culture flasks in a sterile, 37 °C incubator with a humidified atmosphere supplemented to 5% CO_2 and passaged 1:3 when they reached 75-90% confluence, with media otherwise replaced every other day. Primary cells were used at passages less than 9. The embryonic rat aortic smooth muscle cell line A7r5 was also used for TEM and confocal studies. A7r5, HEK 239T, and their stable derivatives were grown in DMEM

supplemented with 10% FBS, 1% penicillin-streptomycin, and 1x ciprofloxacin (GenHunter, Nashville, TN, USA), and supplemented as noted with selection antibiotics to select cells expressing transgenes.

Flow Cytometry Quantification of Peptide Uptake Inhibition

Flow cytometry was performed as previously reported[19], except that before treatment with MK2i-NPs or MK2i peptide, HCAVSMCs were pre-treated with endocytic inhibitors for 30 minutes, before being co-treated with inhibitor and mk2i-NP or peptide treatment. Doses for these inhibitors were verified to be above the published IC_{50} literature values, consistent with other published inhibition studies, and to be in a range that did not cause significant toxicity in our hands in HCAVSMC pilot studies. Briefly, cells were seeded in triplicate in a 24 well plate at 30,000 cells *per* well and allowed to adhere overnight. Cell culture media was replaced with OptiMEM supplemented with 1% FBS, 1% penn-strep, and appropriate doses of each small molecule inhibitor: dynamin, 50 or 100 nM; Nystatin, 50 μg/mL; methyl-β-cyclodextrin, 5 mM; cytochalasin D, 5 μM; 5-(N-ethyl-N-isopropyl)amiloride (EIPA), 50 μM; wortmannin, 10, 50, and 100 nM; amiloride, 50 μM; polyinosinic acid, 50 μg/mL; and dextran sulfate, 100 μg/mL. Fluorescently labeled MK2i-NPs (10 μM) or free MK2i peptide (10 μM) were added to co-treat the cells for 30 minutes. Cells were then washed twice with PBS -/-, trypsinized, and resuspended in 0.1% Trypan blue in PBS (to quench extracellular fluorescence) for analysis on a FACSCalibur flow cytometer equipped with BD CellQuest Pro software (v 5.2). Data was exported and analyzed with FlowJo software (V 7.6.4). Mean fluorescence intensity (MFI) was calculated by gating the cell population *via* forward and side scatter and subtracting the baseline MFI of untreated cells. Relative uptake was calculated by the following equation where $MFI_{Inhibition}$ and $MFI_{No\ Inhibitor}$ are the mean fluorescence intensities calculated for cells pre-treated with inhibitors and solely treated with

MK2i-NPs or MK2i peptide, respectively:

$$\text{Relative Uptake} = \left(\frac{MFI_{Inhibition}}{MFI_{No\ Inhibitor}}\right) \qquad \text{Eq. 1}$$

Confocal Microscopy

Cells were plated at low confluence (4,000-10,000 cells/well) on an 8-well Nunc Lab-Tek chambered coverslip for confocal microscopy studies. For time course experiments, cells were maintained in a heated chamber with a humidified atmosphere and supplemented with 25 mM HEPES to provide physiologic pH buffering. Confocal image analysis was performed using the Nikon C1si+ system on a Nikon Eclipse Ti-0E inverted microscopy base, Plan Apo VC 20x differential interference contrast N2 objective, 0.75NA, Galvano scanner, and 408/488/543 dichroic mirror. The PMT HV gain, laser power, and display settings were set for maximal SNR based on control biological samples such that negative control samples lacking label had no background fluorescence and positive control samples had no saturated pixels. To ensure no crosstalk between fluorophores, image were acquired sequentially line by line (i.e., line 1 was imaged first with 405 ex / 450 em, then with 488 ex / 515 em before proceeding to line 2). Lack of crosstalk was verified with fluorescence-minus-one controls for all fluorescence channels. Nikon Perfect Focus System was used to ensure image focus. Image acquisition and analysis were performing using Nikon NIS-Elements AR version 4.30.01.

Scanning Electron Microscopy Imaging of Cellular Membrane Morphology

Samples were fixed in 2.5% gluteraldehyde in 0.1M cacodylate buffer (pH 7.4) at 37ºC for 1 hour and then transferred to 4ºC overnight. The samples were washed in 0.1M cacodylate buffer, incubated for 1 hour in 1% osmium tetraoxide at room temperature (RT), and then washed with 0.1M cacodylate buffer. Subsequently, the samples were dehydrated through a graded ethanol series followed by 3 exchanges of 100% ethanol. Samples were then critical point dried on a

Tousimis samdri-PVT-3D critical point dryer and mounted on carbon adhesive attached to aluminum stubs. Samples were then sputter coated with gold/palladium for 90 seconds. Images were taken on FEI Quanta Q250 SEM.

Transmission Electron Microscopy Imaging of Cellular Uptake and Trafficking

Samples were fixed in 2.5% gluteraldehyde in 0.1M cacodylate buffer, pH7.4 at 37ºC for 1 hour then transferred to 4ºC, overnight. The samples were washed in 0.1M cacodylate buffer, then incubated 1 hour in 1% osmium tetraoxide at RT then washed with 0.1M cacodylate buffer. Subsequently, the samples were dehydrated through a graded ethanol series, followed by 3 exchanges of 100% ethanol and 2 exchanges of pure propylene oxide (PO). Dehydrated samples infiltrated with 25% Epon 812 resin and 75% PO for 30 minutes at RT, followed by infiltration with Epon 812 resin and PO [1:1] for 1 hour at RT and subsequent infiltration with fresh Epon 812 resin and PO [1:1] overnight at RT. The samples were subsequently infiltrated with resin for 48 hours and then allowed to polymerize at 60°C for 48 hours. Samples were cut to 500 - 1000 nm thick sections using a Leica Ultracut microtome. Thick sections were contrast stained with 1% toluidine blue and imaged with a Nikon AZ100 microscope to locate cells. 70-80 nm ultra-thin sections were cut and collected on 300-mesh copper grids and then post-stained with 2% uranyl acetate followed by Reynold's lead citrate. Thin samples were imaged on a Philips/FEI Tecnai T12 electron microscope.

Generation of Stably Transfected Cell Lines

Retroviral transfer plasmids encoding galectin/yellow fluorescent protein fusion proteins were kindly gifted by Felix Randow[43]. The retroviral packaging and pseudotyping vectors pUMVC and pCMV-VSV-G (Addgene.com Plasmid #8449 and #8454, respectively) were kind gifts of Bob Weinberg[42]. Galectin-YPF, pUMVC, and pCMV-VSV-G (9:8:1 mass ratio) were transfected into

HEK 239T cells at 50% confluence in T-75 plates using Fugene 6 according to the manufacturer's instructions to produce pseudotyped MMLV retroviral particles. Cell culture media was changed after 24 hours; viral supernatant collected between hours 24-48 and 48-72 hours post-transfection were syringe filtered and frozen at -20 °C until use. A7r5 cells were transduced overnight with 1:10 (v/v) viral supernatant:media and allowed to incubate for 24 hours, at which point cells were transferred into selection media containing Blasticidin (10 μg/ml). After 2 weeks, cells were plated by limiting dilution for single clonal selection and expansion to ensure homogenous expression levels for downstream assays. Successful selection was validated by fluorescence microscopy using non-transfected cells as a control.

Time Lapse Galectin 8 Microscopy

Single cell clonal populations were plated at 5,000 cells/well in chambered coverslips as described for confocal microscopy. Cells were monitored for 3-5 minutes to establish baseline Galectin 8 fluorescence. Cells were then treated for 30 minutes, after which the media was replaced. Live imaging was continued post-wash for at least 3 hours. Images were processed using the "spot detection" algorithm within Nikon NIS-Elements AR version 4.30.01 (Build 1021) and exported to Prism GraphPad and normalized to pre-treatment baseline fluorescence.

Statistics

Statistical analysis was performed *via* one-way ANOVA followed by Tukey's post-hoc test to compare experimental groups. Analyses were done with Microsoft Excel or Graphpad Prism 6 software. Statistical significance was accepted within a 95% confidence limit with a significance level of $\alpha = 0.05$. Results are presented as arithmetic mean ± SEM graphically. For time-lapse galectin 8 recruitment data, statistical significance was defined by non-overlapping 95% confidence intervals.

RESULTS

Characterization of Cellular Uptake Mechanisms

To confirm that the A7r5 rat aortic smooth muscle cell line recapitulates the uptake behavior of human coronary artery smooth muscle cells as previously reported[18,19], A7r5 cells were treated with 10 μM fluorescently labeled MK2i-NPs or MK2i peptide. MK2i-NP and MK2i treated cells both show higher mean fluorescence intensity relative to no treatment cells, and MK2i-NP treated A7r5 cells show a 49-fold increase in MFI compared to cells treated with free MK2i peptide (**Fig. 1b**). These data recapitulate our previous results and validate that formulation of therapeutic CPPs into NPs increases peptide uptake by over an order of magnitude in vascular smooth muscle cells. To confirm these differences qualitatively, we visualized cell peptide uptake by fluorescence confocal microscopy (**Fig. 1c** and **1d**).

Figure 1.

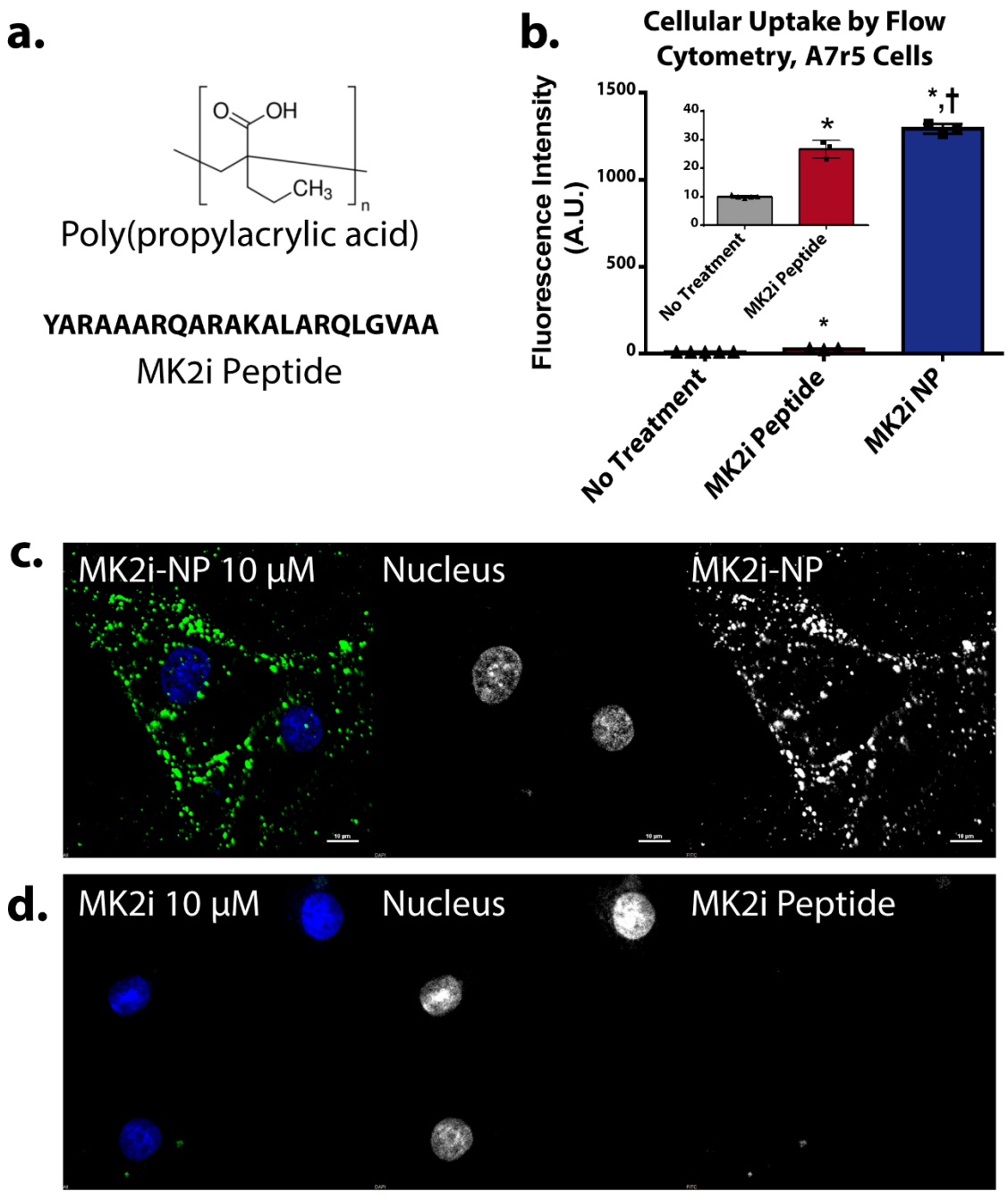

MK2i-NP and MK2i are displayed with equal display settings.

Figure 1. NP formulation of MK2i peptide significant enhances cell internalization in A7r5 VSMCs. *(a) Chemical structure of poly(propylacrylic acid) and sequence of MK2i peptide. (b) Flow cytometric mean fluorescence intensity of cells treated with fluorophore-labeled 10 µM MK2i peptide either as free peptide or formulated into MK2i-NPs. (c, d). Fluorescence microscopy images of A7r5 cells after 30 minutes of treatment with 10 µM MK2i-NP or MK2i peptide; scale bar is 10 µm; blue is nuclei, green is labeled MK2i peptide*

To further understand the effects of NP formulation on MK2i uptake, a library of small molecule inhibitors of different endocytic pathways was used (see inhibitor descriptions in **Table 1**). Specifically, we sought to investigate: macropinocytosis, which has been implicated in CPP and nanoparticle internalization[26] and can be upregulated by cell surface receptor crosslinking[20,38]; clathrin- and caveolin mediated endocytosis, which has been implicated in MK2i internalization[10,22]; lipid raft mediated endocytosis[10], which has been implicated in MK2i internalization in some cell types; and scavenger receptor mediated uptake, which is known to be highly utilized in smooth muscle cells for uptake of negatively charged, hydrophobic particles like low-density lipoprotein that have similar physicochemical properties to PPAA-based MK2i-NPs[9,11,31].

Table 1.Selected inhibitors of endocytosis

Inhibitor	Pathway Inhibited	Mechanism
Wortmannin[20]	Macropinocytosis, phagocytosis	an inhibitor of phosphatidylinositol-4,5-bisphosphate 3-kinase [PI3K], which is required for closure of macropinosomes
Cytochalasin D[37]	Macropinocytosis, phagocytosis	an inhibitor of actin polymerization, which is required for membrane ruffling and macropinosome formation
5-(N-Ethyl-N-isopropyl)amiloride (EIPA) [29]	Macropinocytosis	inhibitor of Rac1/Cdc42 signaling that is required for macropinocytosis
Dynasore[34,46]	Clathrin mediated endocytosis, caveolin mediated endocytosis	an inhibitor of dynamin, a GTPase responsible for clathrin mediated endocytosis, caveolin mediated endocytosis, and the related lipid raft mediated endocytosis
Nystatin[48]	Lipid raft mediated endocytosis	a molecule that binds to and sequesters membrane cholesterol thereby inhibiting lipid raft mediated endocytosis
Methyl-β-cyclodextrin[48]	Lipid-raft mediated endocytosis	Chelates plasma membrane cholesterol, thereby inhibiting lipid-raft mediated endocytosis
Polyinosinic acid[9]	Scavenger receptor mediated endocytosis	Depletes cell surface of scavenger receptors by saturating binding and causing receptor internalization; competitive agonist
Dextran Sulfate ($DxSO_4$) [9]	Scavenger receptor mediated endocytosis	Depletes cell surface of scavenger receptors by saturating binding and causing receptor internalization; competitive agonist

Both MK2i-NP and MK2i peptide uptake were significantly inhibited by dynasore, indicating that clathrin and/or caveolae mediated endocytosis plays a key role in their uptake, consistent with the results previously reported by Brugnano and colleagues for MK2i peptide uptake (which they denote "YARA")[10]. Uptake of MK2i-NPs, but not MK2i, was significantly inhibited by all inhibitors implicated in macropinocytosis (i.e., wortmannin, cytochalasin D, and EIPA). We initially hypothesized that scavenger receptors may play a role in MK2i-NP and/or MK2i uptake due to their negative and positive charge, respectively[5,9,11,31]. However, treatment with the scavenger receptor inhibitors polyinosinic acid or dextran sulfate ($DxSO_4$) had no significant effects on MK2i-NP or MK2i uptake. Furthermore, inhibition of lipid-raft systems *via* nystatin or methyl-β-cyclodextrin pretreatment also showed no significant effects on MK2i-NP or MK2i uptake. Collectively, these data suggest that MK2i-NPs are internalized through macropinocytic mechanisms in addition to the clathrin- and or caveolae mediated endocytic mechanisms responsible for uptake of the free MK2i peptide. The modest (and not statistically significant) increases in internalization of MK2i peptide with wortmannin, cytochalasin D, EIPA, and nystatin treatment are likely due to compensatory uptake mechanisms as previously shown by Brugnano et al.[10]

Figure 2.

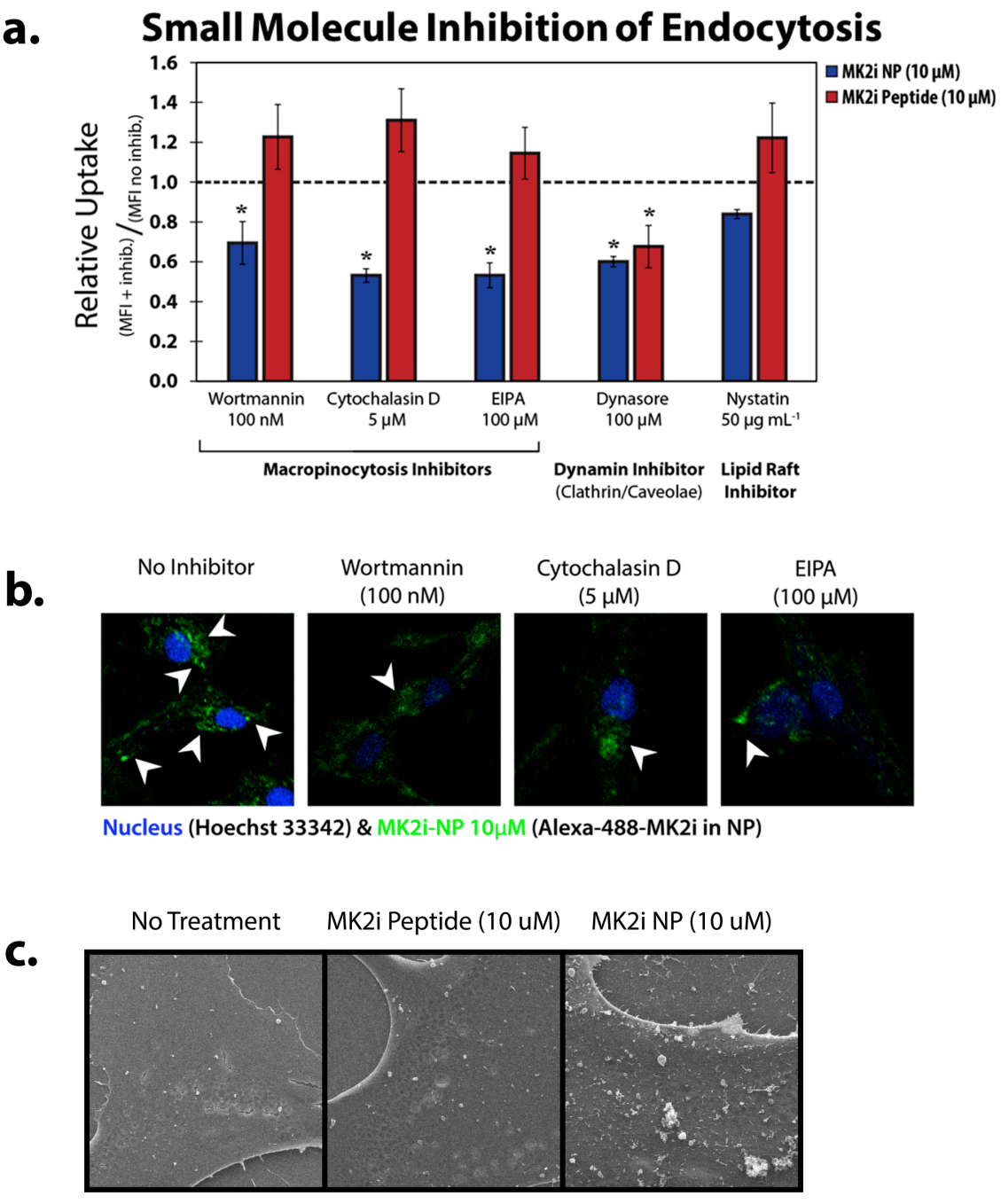

Figure 2. MK2i-NPs enter cells through macropinocytosis while free MK2i exclusively utilizes clathrin mediated endocytosis. *(a) Uptake inhibition of macropinocytosis, dynamin, and lipid rafts as measured by flow cytometry. Data is presented as mean fluorescence intensity relative to no treatment control. (b) Confocal micrographs of cells treated with MK2i-NP 10 μM and macropinocytosis inhibitors (c) scanning electron micrographs showing induction of cell surface ruffling indication macropinocytosis of MK2i-NPs*

To confirm these results, live cells were treated with macropinocytosis inhibitors and visualized through confocal microscopy imaging (**Fig. 2b**). Cells treated with any of the macropinocytosis inhibitors showed a marked decrease in the amount of large / macropinosome-like vesicles positive for MK2i-NP fluorescence (white arrows in **Fig. 2b**). Because macropinocytosis is a process that involves re-organization of the actin cytoskeleton to form membrane protrusions (i.e., pseudopodia and membrane ruffling / blebbing) (**Fig. 3**) that engulf extracellular fluid, we sought to visualize this mechanism by SEM as previously reported[36]. Cells

Figure 3.

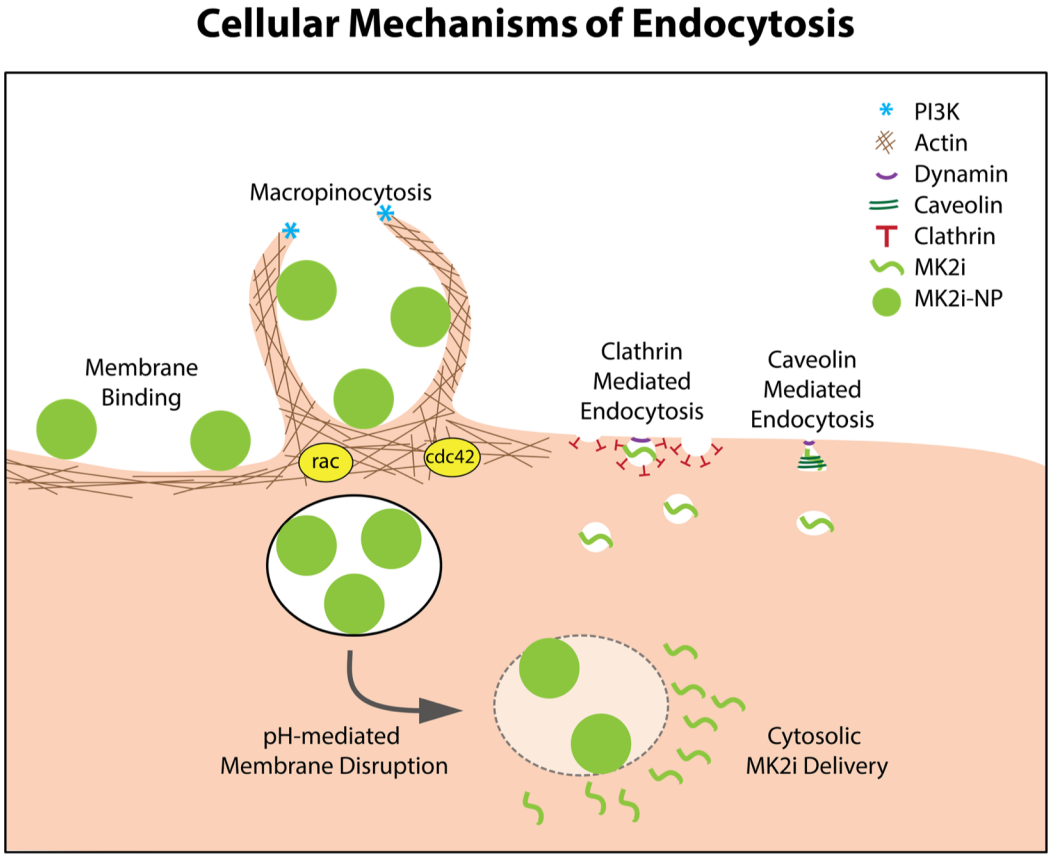

Figure 3. Mechanisms of endocytosis. *Macropinocytosis is a process of nonspecific internalization of large amounts of extracellular fluid characterized by actin-rich protrusions from the cell surface which close in a phosphoinositide 3-kinase (PI3K) dependent step and rely on Rac/Cdc42 signaling. Clathrin mediated endocytosis and caveolin mediated endocytosis rely on a dynamin dependent closure step for internalization. MK2i-NP is proposed to enhance uptake by binding to external plasma membrane and internalize via macropinocytosis*

were treated with 10 μM MK2i-NPs, MK2i, or PBS. As expected, MK2i-NPs, but not MK2i or PBS, induced a high degree of visible membrane ruffling (**Fig. 2c**).

Transmission Electron Microscopy

TEM imaging was utilized for high resolution visualization of cellular ultrastructure during uptake and intracellular trafficking of gold-labeled MK2i-NPs (Au-MK2i-NPs). Au-MK2i-NP size equivalence with MK2i-NPs and gold loading (~98%) were confirmed by dynamic light scattering (DLS, **Fig. S2**). Gold-labeled MK2i peptide was excluded from TEM studies because of concerns that 10 nm gold would significantly affect trafficking of the individual peptide molecules, which are very small relative to the gold (i.e., 2 nm compared to 10 nm diameters for the peptide and gold, respectively). Furthermore, irreversible aggregation and precipitation were apparent upon mixing of the gold label with free MK2i peptide. Therefore, free gold was used as a control. Samples were treated for 30 minutes and thoroughly washed 1x with media and 5x with PBS. Samples were then either immediately fixed or incubated in fresh media for an additional 24 hours prior to fixation and processing.

TEM imaging shows that Au-MK2i-NPs are visibly clustered at the plasma membrane during uptake in cells fixed immediately after 30 minutes of treatment (**Fig. 4.a.i. & 4.a.ii.**). TEM images evinced structures consistent with macropinocytosis (**Fig. 4.a.iii & 4.a.iv.**), which were not found in untreated or gold only samples (**Fig. 4.d.i. & 4.d.iii.**). Au-MK2i-NPs are also found both contained within vesicular structures (**Fig. 4.b.**, black arrows) and in the cytosol at 30 minutes (**Fig. 4.b.ii. & 4.b.iv.**, white arrows). At 24 hr. post-treatment, Au-MK2i-NPs are found within the cell both inside vesicular structures consistent with the endo-lysosomal system (**Fig. 4.c.i.-iii.**, black arrows) and outside membrane bound vesicles (**Fig. 4.c.ii-iv.**, white arrows), suggesting endosomal escape and cytosolic MK2i delivery. Although some Au-MK2i-NPs were found to

reside within vesicles with clearly visible and intact membranes (**Fig. 4.c.i.**, black arrows), they were also commonly associated with vesicles with disrupted membranes [i.e., only partial membranes (**Fig. 4.c.ii.**, black arrows) or fragmented membranes (**Fig. 4.c.iii.**, all particles)]. These damaged and swollen vesicles found in Au-MK2i-NP treated cells are in clear contrast to untreated or gold only treated control cells (**Figs. 4.d.i-iv.**). These are the first high-resolution electron micrographs, to our knowledge, that enable visualization of the endosomal disruption activity of the highly-utilized endosomolytic polymer PPAA.

Figure 4.

Figure 4a. NP binds to cell membrane, inducing macropinosome formation at t = 30 min.

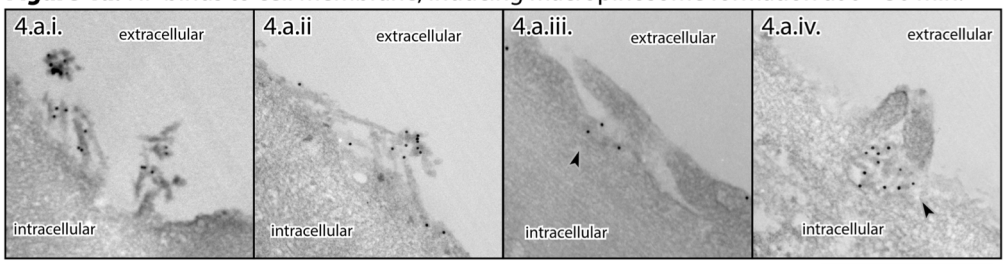

Cells treated 30 minutes with 10 uM Au-MK2i-NP and immediately fixed. 500 nm

Figure 4b. NP found both inside vesicles and in cytosol near vesicles at t = 30 min.

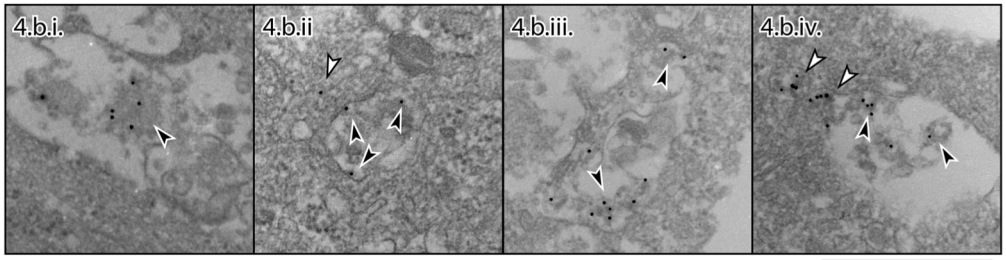

Cells treated 30 minutes with 10 uM Au-MK2i-NP and immediately fixed. 500 nm

Figure 4c. NP found inside vesicles and in cytosol at t = 24 hr.

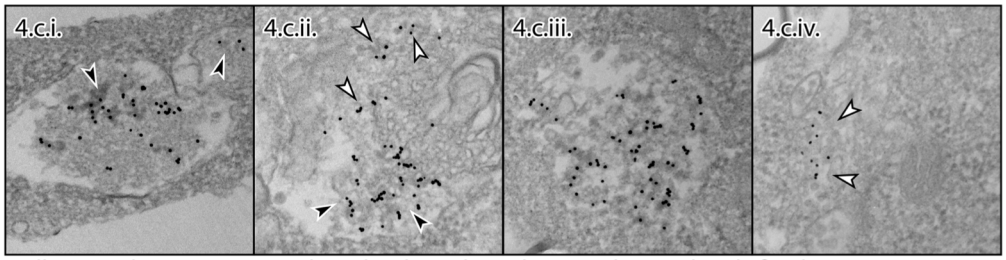

Cells treated 30 minutes, incubated 24 hr with medium, and immediately fixed. 500 nm

Figure 4d. Untreated control cells or gold only control as marked.

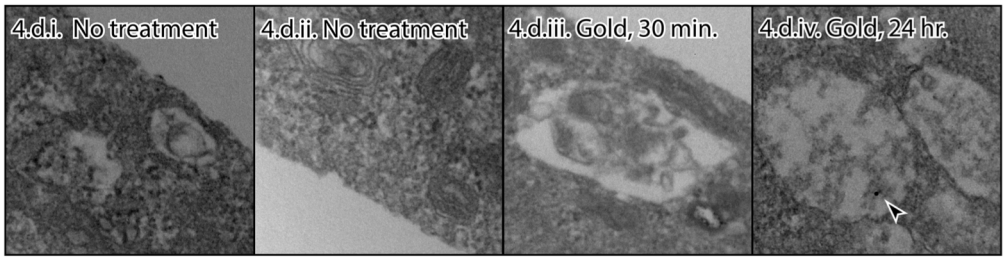

Cells were treated with PBS or dose-matched gold as controls. 500 nm

Key:
Vesicular
Cytosolic

Figure 4. TEM analysis supports MK2i-NP uptake by macropinocytosis and escape from endo-lysosomal vesicles. *(a) Au-MK2i-NP binds to cell membrane, inducing macropinosome formation. (b) Au-MK2i-NP is apparent both inside vesicles and in cytosol near vesicles at t=30 minutes. (c) Au-MK2i-NP are also visualized inside of vesicles and in the cytosol at t=24 hours. (d) Untreated cells and Au-alone treated cells showing lack of membrane binding and low intracellular accumulation.*

Figure 5.

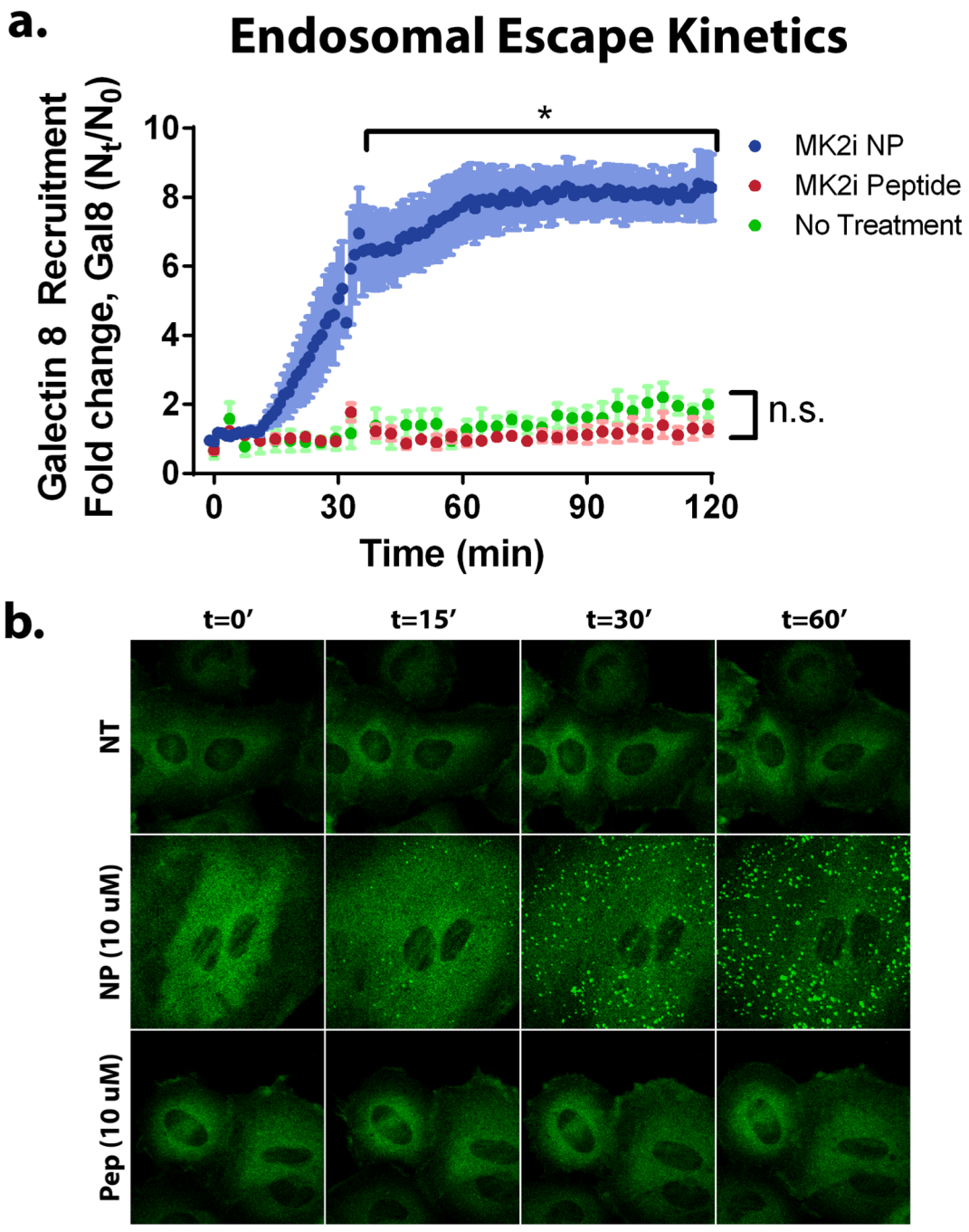

Figure 5. MK2i-NP treatment rapidly triggers endosomal disruption as visualized with Galectin 8 recruitment. *(a) Endosomal disruption kinetics are plotted as fold change in gal8 punctation. From top to bottom, blue circles represent 10 μM MK2i-NP, green circles represent no treatment, and red circles indicate 10 μM MK2i. Treatments were removed at t = 30 minutes and replaced with fresh medium. Asterisk (*) indicates $p < 0.05$ for MK2i-NP vs MK2i and NT. (b) Representative images are shown for no treatment, MK2i-NP 10 μM, and MK2i peptide 10 μM at t = 0, 15, 30, and 60 minutes.*

Real-time Monitoring of Endosomal Escape

To determine the temporal kinetics of endosomal escape revealed by TEM, a novel live-cell fluorescent imaging methodology based on intracellular localization of galectin-8 (Gal8) was performed to assess endosomal membrane damage during MK2i-NP treatment. Gal8 is a β-galactoside-binding lectin of the galectin family, and is normally normally localized diffusely throughout the cytosol and secreted, binding to glycans in the extracellular space to influence cell behavior[1]. They also serve as part of the innate immune to sense exposed intracellular glycans[43], which is relevant to the current application in that glycans are naturally located on the external plasma membrane or enclosed within vesicles (e.g., on the luminal surfaces of endosomes, macropinosomes, etc.). When endosomes are disrupted by pathogens (e.g., bacteria)[43] or transfection reagents (e.g., Lipofectamine)[47], Gal8 binds to glycans on the exposed luminal surface of the endosomal membrane and induces macroautophagy (i.e., sequestration in a *de novo* generated double-membraned autophagosome[8] that fuses with lysosomes to facilitate degradation of the autophagosomal contents). In 2015, Wittrup et al.[47] showed that Lipofectamine lipoplexes induce endosomal damage at the Rab 5 to Rab 7 conversion step, at which point, nucleic acids are released into the cytosol. These studies also showed that the transient leakiness of damaged endosomes results in detectible recruitment of galectin-8 due to accessibility to glycans within the endosomal lumen. Based on this method, A7r5 cells were generated that stably express Gal-8-YFP, enabling real time monitoring and quantification of endosomal disruption in vascular smooth

muscle cells **(Fig. 5a).** Treatment with MK2i-NPs, but not free MK2i peptide, rapidly induced recruitment of Gal8 to intracellular vesicles (bright punctate staining in **Fig. 5b**), whereas treatment with free MK2i peptide showed no appreciable changes over time. We also located, in MK2i-NP-treated cells, double membrane structures consistent with autophagosomes merging with electron dense vesicles consistent with lysosomes 30 minutes after treatment (**Fig. 6**).

Figure 6.

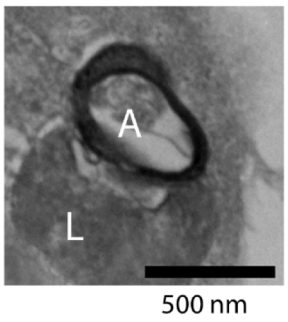

Figure 6. TEM image showing a structure consistent with autophagosome morphology merging with a lysosome.
Time = 30 minutes. L marks electron dense structure consistent with lysosome, A marks a double membrane structure consistent with a damaged vesicle sealed inside an autophagosome µM MK2i peptide.

DISCUSSION

This work focused on investigating the cellular uptake and intracellular trafficking mechanisms of a novel nano-polyplex formulation for the intracellular delivery of a therapeutic, anti-inflammatory MK2 inhibitory peptide. This MK2i-NP formulation was initially developed to circumvent peptide endo-lysosomal sequestration and degradation to increase the intracellular bioavailability of MK2i in vascular smooth muscle cells, thereby increasing potency and longevity of action as a prophylactic approach to improving the patency of vascular bypass grafts. Serendipitously, formulation into NPs was found to significantly increase MK2i peptide uptake in addition to enabling endosomal escape and increasing intracellular half-life. The clinical translatability of the MK2i-NP formulation was then validated in a pre-clinical animal model of bypass grafting, where treatment with MK2i-NPs was found to significantly enhance the ability of the MK2i peptide to prevent intimal hyperplasia in vein transplants *in vivo*[18]. Thus, the studies

herein were designed to gain mechanistic insight into how NP formulation influences the cellular uptake and intracellular trafficking of the MK2i peptide to realize a more effective peptide-based therapy. By elucidating the mechanism of MK2i-NP uptake and trafficking, we can potentially efficacy so that they can be more broadly applied to improve the intracellular delivery of peptides and other biomacromolecular therapeutics.

Flow cytometry based analysis of MK2i-NP uptake verified that NP formulation significantly increased MK2i uptake in A7r5 rat aortic smooth muscle cells 49-fold (**Fig. 1b**), recapitulating the uptake effects found in primary human coronary artery vascular smooth muscle cells. Confocal microscopy imaging revealed that MK2i-NPs strongly associated with the cellular membrane (**Supplemental figure S3**), likely due to interactions of the hydrophobic/lipophilic propyl moiety of the PPAA polymer with the hydrophobic tails of phospholipids in the cellular membrane. To understand if this enhanced membrane association influences the mechanism of cellular internalization, uptake studies were performed in conjunction with a library of small molecule inhibitors of various endocytic pathways. Although the MK2i peptide is positively charged, MK2i-NPs have a negative ζ-potential (i.e., surface charge) due to the relative excess of anionic PPAA polymer (charge ratio of the optimized NP formulation is one positively charged peptidic primary amine on the MK2i peptide to 3 negatively charged polymeric carboxylate groups on PPAA). Considering that scavenger receptors are implicated in the uptake of negatively charged, oxidized low-density lipoprotein particles in vascular smooth muscle cells[5,31], we initially hypothesized that scavenger receptors may be responsible for the observed increase in peptide uptake. However, two separate scavenger receptor inhibitors, polyinosinic acid and dextran sulfate, were found to have no influence on MK2i-NP uptake. In agreement with previous studies[10,22], uptake of the MK2i peptide appeared to be dependent on clathrin- and/or caveolae mediated

endocytosis and independent of macropinocytosis. In contrast, MK2i-NP uptake was found to be dependent on both macropinocytosis and clathrin- and/or caveolae mediated endocytosis.

Electron microscopy studies confirmed that macropinocytosis as an underlying mechanism of enhanced uptake of MK2i-NPs. SEM analysis of MK2i-NP treated cells confirm the induction of macropinocytosis as evinced by appearance of membrane ruffling, blebbing, and protrusions that were not present in untreated cells or cells treated with the free MK2i peptide (**Fig. 2c**). TEM analysis further supported macropinocytosis as a differential mechanism of MK2i-NP uptake. Gold-labeled Au-MK2i-NPs were found to strongly associate with areas of the cell membrane that displayed membrane ruffling, membrane blebbing, and pseudopodia. Furthermore, Au-MK2i-NPs were found within large diameter (i.e., ~500 nm) vesicular compartments consistent with morphology of macropinosomes **(Fig. 4b.i-iv., 4ci-iii.).**

Macropinosomes have been reported to be inherently more leaky than endosomes[27], so we aimed to determine the trafficking and ultimate fate of MK2i-NPs following cellular internalization. Previous studies demonstrated that MK2i-NPs display pH-dependent red blood cell membrane disruption ideally tuned for escape from acidified endo-lysosomal compartments. TEM analysis of Au-MK2i-NP uptake further support that NP formulation enables peptide endosomal escape and cytosolic delivery: TEM images clearly demonstrate Au-MK2i-NPs associated with disrupted intracellular membranes and also show Au-MK2i-NPs in the cytosol of treated cells (i.e., not bound by a plasma membrane) **(Fig. 4b.ii, iv; Fig. 4.c.ii-iv) .** This endosomal escape and cytosolic delivery can be attributed to both the pH-dependent membrane disruptive properties of PPAA and the leakiness of macropinosomes. To further investigate membrane disruption as the mechanism of cytosolic MK2i delivery, a novel assay utilizing A7r5 smooth muscle cells transfected with a stably integrated, fluorescent Galectin 8 reporter was utilized. In

contrast to untreated control cells and cells treated with free MK2i peptide, MK2i-NP cell treatment triggered significant recruitment of Galectin 8 to intracellular vesicles, indicating active membrane disruption. Interestingly, TEM images evinced double membrane autophagosomal structures (**Fig. 5c**) in Au-MK2i-NP treated cells that were not found in control cells consistent with damaged endosomes' altered trafficking to lysosomes. This result is in agreement with Wittrup et al.'s observations[47] that Lipofectamine lipoplexes traffic to autophagosomes following Gal8 recruitment. In turn, Gal8 recruits NDP52 and LC3 proteins that are responsible for the formation of a secondary containment membrane around the damaged endosome[43,47], which is then rapidly trafficked to terminal lysosomes[4,8,23,40]. Our data further supports the importance of identifying the role autophagosomal encapsulation of damaged endosomes plays in the delivery of biomacromolecular therapeutics and may help to explain the discrepancy between the 49-fold enhancement in uptake paired with the approximately 10-fold enhancement in bioactivity. Autophagosomal escape may represent a viable pathway for further enhancement of intracellular bioavailability of biomacromolecules delivered *via* endosomolytic carriers.

In conclusion, our data demonstrate that formulation of a therapeutic MK2i peptide into a slightly hydrophobic, pH-responsive NPs enhances uptake through enhanced cellular membrane association and macropinocytosis. This enhanced membrane association is hypothesized to be a result of the hydrophobic nature of the PPAA polymer causing interactions with lipids in the cell membrane. Furthermore, the pH-responsive behavior of the PPAA polymer results in pH-triggered endo-lysosomal disruption following cellular internalization, observed by TEM as both escape and disruption of membrane morphology. The endosomal disruption of MK2i-NP was further supported by Gal8 recruitment and subsequent trafficking into autophagosomes. Therefore, these studies suggest that formulation of MK2i into NPs significantly increases peptide uptake and

facilitates endosomal escape by influencing both the mechanism of cellular uptake and intracellular trafficking. Endosomal escape not only prevents endo-lysosomal degradation and/or exocytosis *via* recycling endosomes, but also increases intracellular bioavailability. These studies suggest that macropinocytosis may be a very efficient route of entry for biologic drugs and that macropinosomes can be escaped by endosomolytic carriers. Further, Gal8 recruitment may be a useful assay for identifying critical structure-function relationships between nano-scale drug delivery carriers and bioactivity, and may prove useful in screening the endosomolytic properties of nanoscale drug carriers. We show that endosomolytic carriers still suffer from partial lysosomal entrapment due to autophagosomal encapsulation of damaged endosomes followed by lysosomal trafficking. This result suggests that autophagosomal trafficking and sequestration may be another critical barrier in the delivery of cytosolic therapeutics; inhibiting this process may represent a high potential target for further enhancements to intracellular bioavailability of cytosolic-acting biologic therapeutics.

Finally, further research into the structure-function relationships of peptide nano-polyplexes is warranted. PPAA has been shown to be applicable to multiple peptides[19], though it is unknown whether PPAA alters intracellular trafficking for all biomacromolecular cargo in similar manner. Efficient delivery of protein and peptide drugs to cytosolic targets remains a critical barrier in the clinical translation of cytosol acting peptide drugs. Even the strongest endosomolytic agents are only partially efficient at cytosolic delivery and endosomal escape and may be limited in their delivery efficiency by autophagosome sequestration mechanisms.

REFERENCES

1. Barondes, S.H., D.N. Cooper, M.A. Gitt, and H. Leffler. Galectins. Structure and function of a large family of animal lectins. *J. Biol. Chem.* 269:20807–20810, 1994.

2. Behr, J.P. The proton sponge: a trick to enter cells the viruses did not exploit. *CHIMIA International Journal for Chemistry* 51:34–36, 1997.

3. Berguig, G.Y. *et al.* Intracellular delivery and trafficking dynamics of a lymphoma-targeting antibody-polymer conjugate. *Mol. Pharm.* American Chemical Society, 9:3506–3514, 2012.

4. Bernard, A., and D.J. Klionsky. Toward an understanding of autophagosome-lysosome fusion: The unsuspected role of ATG14. *Autophagy* 11:583–584, 2015.

5. Bickel, P.E., and M.W. Freeman. Rabbit aortic smooth muscle cells express inducible macrophage scavenger receptor messenger RNA that is absent from endothelial cells. *J. Clin. Invest.* American Society for Clinical Investigation, 90:1450–1457, 1992.

6. Borsello, T. *et al.* A peptide inhibitor of c-Jun N-terminal kinase protects against excitotoxicity and cerebral ischemia. *Nature Medicine* Nature Publishing Group, 9:1180–1186, 2003.

7. Boussif, O. *et al.* A versatile vector for gene and oligonucleotide transfer into cells in culture and in vivo: polyethylenimine. *PNAS* National Acad Sciences, 92:7297–7301, 1995.

8. Boyle, K.B., and F. Randow. The role of "eat-me" signals and autophagy cargo receptors in innate immunity. *Curr. Opin. Microbiol.* 16:339–348, 2013.

9. Brown, M.S., S.K. Basu, J.R. Falck, Y.K. Ho, and J.L. Goldstein. The scavenger cell pathway for lipoprotein degradation: Specificity of the binding site that mediates the uptake of negatively-charged LDL by macrophages. *Journal of Supramolecular Structure* Alan R. Liss, Inc, 13:67–81, 1980.

10. Brugnano, J., J. McMasters, and A. Panitch. Characterization of endocytic uptake of MK2-inhibitor peptides. *J. Pept. Sci.* 19:629–638, 2013.

11. Canton, J., D. Neculai, and S. Grinstein. Scavenger receptors in homeostasis and immunity. *Nat Rev Immunol* 13:621–634, 2013.

12. Convertine, A.J., D.S.W. Benoit, C.L. Duvall, A.S. Hoffman, and P.S. Stayton. Development of a novel endosomolytic diblock copolymer for siRNA delivery. *Journal of Controlled Release* 133:221–229, 2009.

13. Convertine, A.J., D.S.W. Benoit, C.L. Duvall, A.S. Hoffman, and P.S. Stayton. Development of a novel endosomolytic diblock copolymer for siRNA delivery. *J Control Release* 133:221–229, 2009.

14. Copolovici, D.M., K. Langel, E. Eriste, and Ü. Langel. Cell-penetrating peptides: design,

synthesis, and applications. *ACS Nano* 8:1972–1994, 2014.

15. De Smedt, S.C., J. Demeester, and W.E. Hennink. Cationic Polymer Based Gene Delivery Systems - Springer. *Pharmaceutical Research* 17:113–126, 2000.

16. Deshayes, S., M.C. Morris, G. Divita, and F. Heitz. Cell-penetrating peptides: tools for intracellular delivery of therapeutics. *CMLS, Cell. Mol. Life Sci.* Birkhäuser-Verlag, 62:1839–1849, 2005.

17. Duvall, C.L., A.J. Convertine, D.S.W. Benoit, A.S. Hoffman, and P.S. Stayton. Intracellular delivery of a proapoptotic peptide *via* conjugation to a RAFT synthesized endosomolytic polymer. *Mol. Pharm.* American Chemical Society, 7:468–476, 2010.

18. Evans, B.C. *et al.* MK2 inhibitory peptide delivered in nanopolyplexes prevents vascular graft intimal hyperplasia. *Sci Transl Med* 7:291ra95, 2015.

19. Evans, B.C., K.M. Hocking, K.V. Kilchrist, E.S. Wise, C.M. Brophy, and C.L. Duvall. Endosomolytic Nano-Polyplex Platform Technology for Cytosolic Peptide Delivery To Inhibit Pathological Vasoconstriction. *ACS Nano* 9:5893–5907, 2015.

20. Falcone, S., E. Cocucci, P. Podini, T. Kirchhausen, E. Clementi, and J. Meldolesi. Macropinocytosis: regulated coordination of endocytic and exocytic membrane traffic events. *J Cell Sci* The Company of Biologists Ltd, 119:4758–4769, 2006.

21. Felgner, J.H. *et al.* Enhanced gene delivery and mechanism studies with a novel series of cationic lipid formulations. *J. Biol. Chem.* American Society for Biochemistry and Molecular Biology, 269:2550–2561, 1994.

22. Flynn, C.R. *et al.* Internalization and intracellular trafficking of a PTD-conjugated anti-fibrotic peptide, AZX100, in human dermal keloid fibroblasts. *J Pharm Sci* 99:3100–3121, 2010.

23. Furuta, N., and A. Amano. SNARE mediates autophagosome–lysosome fusion. *Journal of Oral Biosciences* 54:83–85, 2012.

24. Gump, J.M., and S.F. Dowdy. TAT transduction: the molecular mechanism and therapeutic prospects. *Trends in Molecular Medicine* Elsevier, 13:443–448, 2007.

25. Hayess, K., and R. Benndorf. Effect of protein kinase inhibitors on activity of mammalian small heat-shock protein (HSP25) kinase. *Biochemical Pharmacology* 53:1239–1247, 1997.

26. Kaplan, I.M., J.S. Wadia, and S.F. Dowdy. Cationic TAT peptide transduction domain enters cells by macropinocytosis. *Journal of Controlled Release* 102:247–253, 2005.

27. Khalil, I.A., K. Kogure, H. Akita, and H. Harashima. Uptake pathways and subsequent intracellular trafficking in nonviral gene delivery. *Pharmacol Rev* American Society for Pharmacology and Experimental Therapeutics, 58:32–45, 2006.

28. Knighton, D.R., J.H. Zheng, L.F. Ten Eyck, N.H. Xuong, S.S. Taylor, and J.M. Sowadski.

Structure of a peptide inhibitor bound to the catalytic subunit of cyclic adenosine monophosphate-dependent protein kinase. *Science* American Association for the Advancement of Science, 253:414–420, 1991.

29. Koivusalo, M. *et al.* Amiloride inhibits macropinocytosis by lowering submembranous pH and preventing Rac1 and Cdc42 signaling. *J Cell Biol* Rockefeller Univ Press, 188:547–563, 2010.

30. Kotlyarov, A. *et al.* Distinct Cellular Functions of MK2. *Molecular and Cellular Biology* American Society for Microbiology (ASM), 22:4827–4835, 2002.

31. Li, H., M. Freeman, and P. Libby. Regulation of smooth muscle cell scavenger receptor expression in vivo by atherogenic diets and in vitro by cytokines. *Journal of Clinical Investigation*, 1995. Available from: http://www.ncbi.nlm.nih.gov/pmc/articles/PMC295387/.

32. Lopes, L.B. *et al.* Cell Permeant Peptide Analogues of the Small Heat Shock Protein, HSP20, Reduce TGF-β1-Induced CTGF Expression in Keloid Fibroblasts. *Journal of Investigative Dermatology* 129:590–598, 2008. Available from: http://www.nature.com/doifinder/10.1038/jid.2008.264.

33. Lopes, L.B., C. Flynn, P. Komalavilas, A. Panitch, C.M. Brophy, and B.L. Seal. Inhibition of HSP27 phosphorylation by a cell-permeant MAPKAP Kinase 2 inhibitor. *Biochemical and Biophysical Research Communications* 382:535–539, 2009.

34. Macia, E., M. Ehrlich, R. Massol, E. Boucrot, C. Brunner, and T. Kirchhausen. Dynasore, a cell-permeable inhibitor of dynamin. *Dev. Cell* 10:839–850, 2006.

35. Meng, W. *et al.* Structure of Mitogen-activated Protein Kinase-activated Protein (MAPKAP) Kinase 2 Suggests a Bifunctional Switch That Couples Kinase Activation with Nuclear Export. *J. Biol. Chem.* American Society for Biochemistry and Molecular Biology, 277:37401–37405, 2002.

36. Mercer, J., and A. Helenius. Virus entry by macropinocytosis. *Nat. Cell Biol.* 11:510–520, 2009.

37. Nakase, I. *et al.* Cellular uptake of arginine-rich peptides: roles for macropinocytosis and actin rearrangement. *Mol. Ther.* 10:1011–1022, 2004.

38. Nakase, I., N.B. Kobayashi, T. Takatani-Nakase, and T. Yoshida. Active macropinocytosis induction by stimulation of epidermal growth factor receptor and oncogenic Ras expression potentiates cellular uptake efficacy of exosomes. *Scientific Reports* Nature Publishing Group, 5:10300, 2015.

39. Richard, J.P. *et al.* Cell-penetrating peptides. A reevaluation of the mechanism of cellular uptake. *J. Biol. Chem.* American Society for Biochemistry and Molecular Biology, 278:585–590, 2003.

40. Shibutani, S.T., and T. Yoshimori. Autophagosome formation in response to intracellular

bacterial invasion. *Cell. Microbiol.* 16:1619–1626, 2014.

41. Sorkin, A., and M. von Zastrow. Signal transduction and endocytosis: close encounters of many kinds. *Nat Rev Mol Cell Biol* 3:600–614, 2002.

42. Stewart, S.A. *et al.* Lentivirus-delivered stable gene silencing by RNAi in primary cells. *RNA* 9:493–501, 2003.

43. Thurston, T.L.M., M.P. Wandel, N. von Muhlinen, A. Foeglein, and F. Randow. Galectin 8 targets damaged vesicles for autophagy to defend cells against bacterial invasion. *Nature* 482:414–418, 2012.

44. Varkouhi, A.K., M. Scholte, G. Storm, and H.J. Haisma. Endosomal escape pathways for delivery of biologicals. *J Control Release* 151:220–228, 2011.

45. Verdine, G.L., and G.J. Hilinski. Stapled Peptides for Intracellular Drug Targets. In: Protein Engineering for Therapeutics, Part B Elsevier, 2012, pp. 3–33.

46. Verma, P., A.G. Ostermeyer-Fay, and D.A. Brown. Caveolin-1 induces formation of membrane tubules that sense actomyosin tension and are inhibited by polymerase I and transcript release factor/cavin-1. *Mol. Biol. Cell* 21:2226–2240, 2010.

47. Wittrup, A. *et al.* Visualizing lipid-formulated siRNA release from endosomes and target gene knockdown. *Nat. Biotechnol.* 33:870–876, 2015.

48. Yamaguchi, H., Y. Takeo, S. Yoshida, Z. Kouchi, Y. Nakamura, and K. Fukami. Lipid rafts and caveolin-1 are required for invadopodia formation and extracellular matrix degradation by human breast cancer cells. *Cancer Res.* American Association for Cancer Research, 69:8594–8602, 2009.